Multi-frequency Amplitude Probability Distribution Measurement System and its Application for Electromagnetic Interference Analysis

Yasushi Matsumoto
National Institute of Information and Communications Technology
4-2-4, Nukuikita, Koganei, Tokyo 184-8795, Japan
e-mail: ymatsumoto@nict.go.jp

Abstract

Successful development of FFT-based amplitude probability distribution (APD) measurement system has enabled multi-frequency and real-time measurement of amplitude statistics for fluctuating signals. This opens up new possibilities for measurement in a range of areas, including the nonlinear effect on wide-band stochastic signals, and interference in multi-carrier communication systems. This paper presents an overview of the measuring system and its applications, and provides examples.

1. Introduction

As radio systems and electromagnetic wave applications rapidly proliferate, the potential for interference among such systems is becoming increasingly serious. Measurement and modeling of interfering signals is the first and primary step for realizing coexistence of these systems. Since interfering signals fluctuate in both amplitude and phase in many situations, it is essential to model such interference as a stochastic process. Amplitude probability distribution (APD) is a frequently used term for random signals, and is defined by the exceeding probability the envelope amplitude. APD was originally used to categorize electromagnetic interference (EMI), but recently it has attracted attention as an EMI test method since it was found to have strong correlation with the bit error probability (BEP) of a digital communication system subjected to the interference [1-3]. The International Special Committee on Radio Interference (CISPR) published the specifications of APD measuring receivers for the compliance testing of radiated emissions [4]. However, conventional receivers have a drawback in that measurement must be done at one fixed frequency, without frequency scanning. This is a substantial limitation for analyzing wideband and fluctuating interference. Against this background, we developed a real-time fast Fourier transform (FFT) based multichannel APD measuring system. The paper presents an overview of the system and its applications in the EMC arena.

2. Overview of FFT-based APD Measurement System

Figs. 1 and 2 respectively provide a block diagram and principles of a single-channel APD measuring receiver.

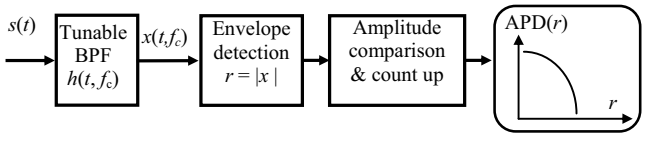

Fig. 1 Single-channel APD measuring receiver

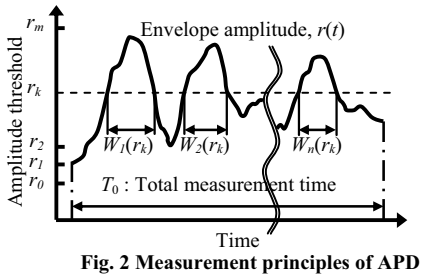

Fig. 2 Measurement principles of APD

The APD at a certain measurement frequency f_c is given by the part of time when the envelope amplitude of the signal r exceeds a threshold value r_k.

$$APD\ (r_k, f_c) \equiv \frac{1}{T_0}\sum_{i=1}^{n(r_k)} W_i(r_k), \quad r(t) \equiv |\, x(t, f_c)\,|, \quad x(t, f_c) \equiv \int_{-\infty}^{\infty} s(t-\tau)h(\tau, f_c)\,d\tau \tag{1}$$

where $s(t)$ denotes the sum of the received signal and receiver noise. The $x(t, f_c)$ represents the bandlimited signal by the receiving filter tuned at f_c (measurement frequency). The $h(t, f_c)$ is the impulse response of the receiving filter, whose bandwidth B defines the receiving bandwidth (or resolution bandwidth). In an FFT-based APD measurement

978-1-4244-6051-9/11/$26.00 ©2011 IEEE

system, the signal $s(t)$ is sampled and input to an N-point FFT, which outputs a set of signal samples, $x(t_j, f_n)$ as follows, each of which corresponds to the bandlimited signal at the frequency of f_n (n=1 to N).

$$x(t_j, f_n) = \frac{1}{N}\sum_{i=1}^{N} s(t_j - i\Delta)w(i\Delta)\exp(j2\pi f_n i\Delta). \quad (2)$$

where Δ is the sampling interval for the FFT, and $1/(N\Delta)$ gives the frequency spacing (f_{n+1}-f_n). The w represents the window function for the FFT, which determines the resolution bandwidth. For each frequency f_n, the envelope amplitude r is calculated and compared to the threshold r_k to obtain the value of APD(r_k, f_n).

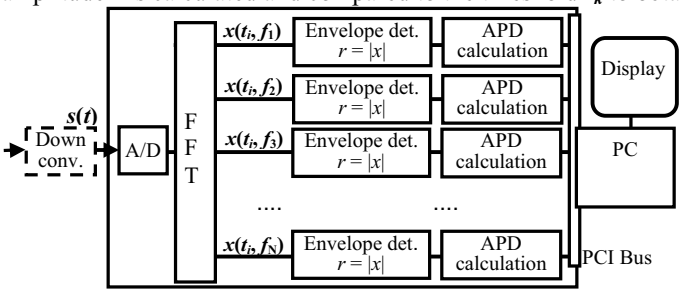

Fig. 3 Construction of the APD measuring system

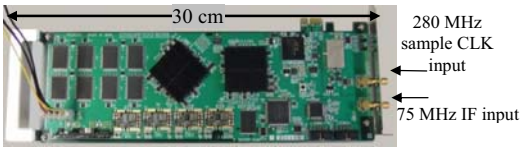

Fig. 4 FPGA board for computation of FFT and APD

Fig. 3 shows the functional diagram of our FFT-based APD measurement system [5]. A field-programmable gate array (FPGA) board (Fig. 4) performs the FFT and computation of APD. The measurement results of APD are sent from the FPGA board to the motherboard of a personal computer (PC) via PCI bus, and displayed in real-time. Note that the RF signal to be measured is down-converted to a 75 MHz IF signal and input to the analog-to-digital converter (ADC). Hence the frequencies f_n (n=1 to N) in Eq. (2) are actually in the IF band, but displayed as those before the down-conversion. The system has three measurement modes, as shown by Table 1.

Table 1 Performance of FFT-based APD measuring system

Measurement mode	DTV	WLAN	CISPR
Number of meas. channels	5617	54	54
Channel separation	0.922 kHz	312.5 kHz	312.5 kHz
Window function	Rectangular	Rectangular	Gaussian
Resolution bandwidth	0.922 kHz	312.5 kHz	1 MHz (impulse BW)
Dynamic range	> 60 dB		
Measurement time	1-120 sec (with dead time less than 1% of the total meas. time)		
Measurement functions	APD, 1st-4th order moments, BEP (estimated with Eq. (4))		

The digital television (DTV) and wireless LAN (WLAN) modes have been developed for estimating the impact of interfering signals on the BEP of DTV and WLAN systems, respectively; both of which are orthogonal frequency division multiplex (OFDM) systems. In these modes, the subchannel bandwidth of APD measurement is the same as that of the OFDM system (DTV or WLAN) to which the BEP estimation is applied [6]. In the DTV mode, an 8192-point FFT with a rectangular window is conducted to generate frequency subchannels spaced by 0.922 kHz that are the same as that in the Integrated Services Digital Broadcasting Terrestrial (ISDB-T) format in Japan. APD measurements in 5617 subchannels are simultaneously conducted in that mode. In the WLAN mode, a 64-point FFT with a rectangular window is performed. APDs can be obtained in 54 subchannels with a bandwidth of 312.5 kHz, which is the same as that of IEEE 802.11g WLAN. Note that unlike usual OFDM receivers, removal of the guard interval is not conducted before the FFT in both modes in order to acquire the entire interference waveform.

In the CISPR mode, on the other hand, the system also conducts a 64-point FFT but with application of a Gaussian window function, which corresponds to a Gaussian receiving filter with an impulse bandwidth of 1 MHz (approximately 0.66 MHz in -3dB bandwidth), which is specified in CISPR16-1-1 for the disturbance measurement above 1 GHz [4]. In this mode, the FFT for the data length of 3.2 μs is performed every 0.4 μs, which means 87.5% overlapped FFT calculations, in order to capture the real peak amplitude when input interference consists of very short pulses. This mode measures the APD with the impulse bandwidth of 1 MHz simultaneously for 64 subchannels spaced by 312.5 kHz. Since the frequency selectivity in this mode is the same as that of conventional CISPR-based measurement methods, it is very effective that the measurement results with this mode can be directly compared with those obtained by conventional methods.

3. Estimation of Interference Impact on OFDM Reception

From the APD of an interfering signal, we can estimate the BEP of a communication system subjected to the interference. Based on the rationale that no symbol errors occur if the envelope amplitude of the interfering signal does not exceed one-half the minimum distance between different signal alternatives, the maximum (worst) BEP of a single-carrier communication system is approximated by [2]

$$P_{b\_\max} \cong \alpha \,\mathrm{APD}\left(\sqrt{\alpha}\beta U\right), \tag{3}$$

where APD(r) represents the amplitude probability distribution of the interfering signal. The U is the root mean square (rms) amplitude of the signal, $1/\alpha$ denotes the number of transmitted bits per symbol, and β is half the normalized minimum signal distance. Values of α and β for typical modulation schemes are presented in [2]. As an example, $\alpha = 1/2$ and $\beta = 1$ for QPSK. The above expression for a single-carrier system can be extended to OFDM systems. The maximum BEP averaged over all OFDM subchannels is expressed by

$$P_{b\_\max} \cong \frac{1}{N}\sum_{n=1}^{N} \alpha_n \,\mathrm{APD}\left(\sqrt{\alpha_n}\beta_n U_n,\ f_n\right). \tag{4}$$

Note that U_n and APD(r, f_n) respectively denote the rms signal amplitude and the APD in subchannel #n. The coefficients α and β for subchannel #n are denoted by α_n and β_n. By applying Eq. (4) to the measurement results of multichannel APD, the degradation in BEP of an OFDM system can be directly estimated. We should note the following conditions must be fulfilled for the application of Eq. (4).

1) Resolution bandwidth of the APD measurement is the same as the subchannel bandwidth of the OFDM system.
2) The noise figure of the APD measurement system is equal to or lower than that of the communication receiver.
3) The communication signal is demodulated with coherent detection and symbol-by-symbol decision.
4) The interfering signal does not affect the frequency or symbol synchronization in the communication receiver.

In order to satisfy condition 1, the DTV and WLAN modes were developed as previously mentioned. A low-noise amplifier is employed for condition 2. Condition 3 is usually satisfied in OFDM systems. For condition 4), we should note that interference may affect the synchronization in actual receivers, which sometimes causes disagreement between the estimated and actual BEP.

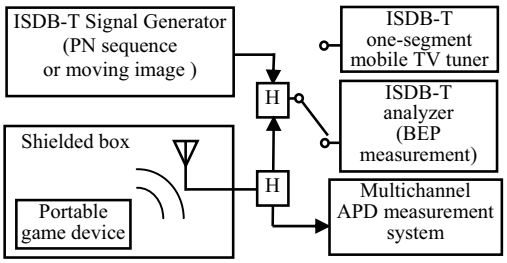

Fig. 5 Evaluation of interference impact on DTV reception

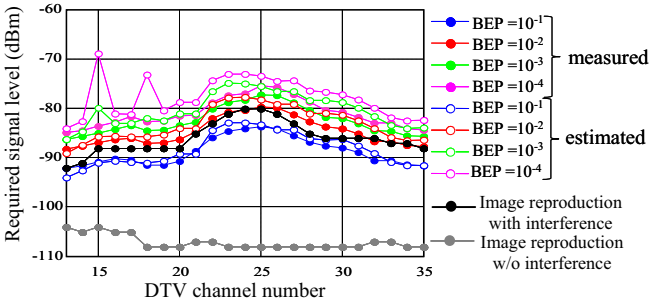

Fig. 6 Estimated and measured DTV signal levels to achieve specific BEPs

We evaluated the impact of a radiated noise from a portable game device on the BEP performance of a one-segment ISDB-T receiver [6]. With the setup shown by Fig. 5, we measured the signal power to achieve given values of BEP in the presence of the noise. The results are plotted as a function of a TV channel number in Fig. 6 (filled circles), and compared with estimated ones from measured APDs (open circles). The estimated results demonstrate good agreement with the measured ones. We also measured the minimum signal levels needed to receive the DTV signal that contained moving images. The minimum signal level for normal reception of the DTV was found to be approximately equal to the signal level in order to achieve BEP of 10^{-2}.

4. Measurement of Nonlinear Effects on DTV Signal

Since OFDM signals consist of a large number of independently modulated subcarriers, they generally have a large peak-to-average power ratio (PAPR). Hence, the OFDM signal is very sensitive to the nonlinearity in the transmission system, and extensive research has been done on nonlinear effects such as intermodulation (IM) products on the quality of transmission (BEP, etc.). By applying APD measurement, we can directly obtain the probability distribution of IM products, from which we can estimate degradation in transmission quality. Figs. 7 and 8 show measured examples of the APD of IM products generated by a nonlinearly amplified ISDB-T signal [5].

Note that the measurement bandwidth is 1 MHz. From the viewpoint of analyzing the impact on BEP, probability distribution of IM products is usually analyzed within an OFDM subchannel bandwidth (0.922 kHz in this case). With the use of the central limit theorem, IM products in one subchannel are commonly approximated as a complex Gaussian noise (i.e., they have the APD of Rayleigh distribution) [7, 8]. However, APDs measured with a wider bandwidth exhibits a heavier-tailed distribution (curve b of Fig. 8) than the Rayleigh distribution (curve a). This point is important when evaluating the impact of the IM products on wideband communication systems.

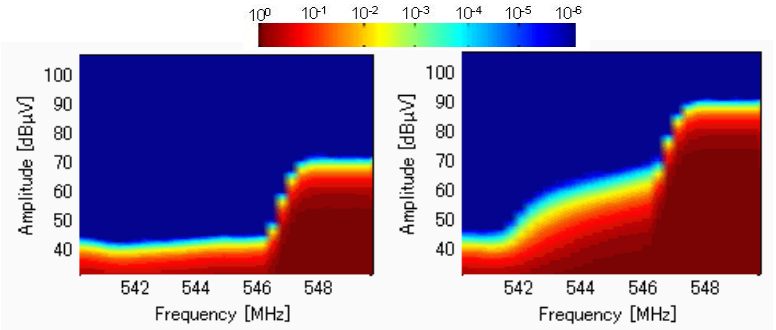

a) Linear operation b) Nonlinear (1 dB compression) operation

Fig. 7 Spectral display of APD for linearly and nonlinearly amplified DTV signals

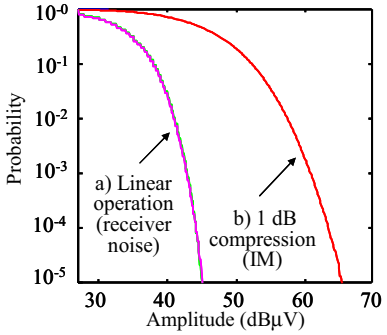

Fig. 8 APD of IM products at 545 MHz (BW= 1 MHz)

5. Conclusion

The FFT-based APD measurement system is a powerful tool for analyzing electromagnetic interference issues in multicarrier communication systems. Degradation in a DTV receiver's sensitivity was demonstrated as being effectively estimated from the APD of an interfering noise. The system was also shown to be useful for analyzing the impact of nonlinearity in OFDM transmission systems.

6. References

1. Y. Yamanaka and T. Shinozuka, "Measurement and estimation of BER degradation of PHS due to electromagnetic disturbance from microwave ovens," *Trans. IEICE*, **J79-B-II**, Nov. 1996, pp. 827-834.

2. K. Wiklundh, "Relation between the amplitude probability distribution of an interfering signal and its impact on digital radio services," *IEEE Trans. on EMC*, **48**, Aug. 2006, pp. 537-544.

3. Y. Matsumoto, "On the relation between the amplitude probability distribution of a noise and bit error probability," *IEEE Trans. on EMC*, **49**, Nov. 2007, pp. 940-941.

4. CISPR 16-1-1 amd. 1, ed. 1, "Specification for radio disturbance and immunity measuring apparatus and methods, Part 1-1: Radio disturbance and immunity measuring apparatus and methods," International Special Committee on Radio Interference, June 2005.

5. K. Gotoh, S. Ishigami, Y. Matsumoto, M. Ryoshi, J. Nishio, and S. Yoshimura, "Development and its application of FFT-based multi-channel APD measuring equipment," *Proc. EMC Europe 2010*, Wroclaw, Sept. 2010, pp. 46-51.

6. K. Gotoh, Y. Matsumoto, H. Tsutagaya, and S. Kazama, "Evaluation of sensitivity of digital TV receiver subjected to intrasystem interference," *Proc. EMC Europe 2008*, Hamburg, Sept. 2008, pp. 727-730.

7. N. Y. Ermolova, "Nonlinear amplifier effects on clipped-filtered multicarrier signals," *IEE Proceedings Communications*, **153**, 2006, pp. 213-218.

8. M. O'Droma, L. Yiming;, E. Bertran, and P. Gilabert, "Analysis of inter-modulation products and nonlinear distortion in RF OFDM transmitter systems," 2009 IEEE 69th Vehicular Technology Conference, Barcelona, April 2009.